# Colorimetric detection of DNA, small molecules, proteins, and ions using unmodified gold nanoparticles and conjugated polyelectrolytes

Fan Xia[a,b,1], Xiaolei Zuo[b,1], Renqiang Yang[c], Yi Xiao[b], Di Kang[b], Alexis Vallée-Bélisle[b], Xiong Gong[a], Jonathan D. Yuen[a], Ben B. Y. Hsu[a], Alan J. Heeger[a,2], and Kevin W. Plaxco[b,2]

[a]Center for Polymers and Organic Solids, and [b]Department of Chemistry and Biochemistry, University of California, Santa Barbara, CA 93106; and [c]Qingdao Institute of Bioenergy and Bioprocess Technology, Chinese Academy of Sciences, 189 Songling Road, Qingdao 266101, China

We have demonstrated a novel sensing strategy employing single-stranded probe DNA, unmodified gold nanoparticles, and a positively charged, water-soluble conjugated polyelectrolyte to detect a broad range of targets including nucleic acid (DNA) sequences, proteins, small molecules, and inorganic ions. This nearly "universal" biosensor approach is based on the observation that, while the conjugated polyelectrolyte specifically inhibits the ability of single-stranded DNA to prevent the aggregation of gold-nanoparticles, no such inhibition is observed with double-stranded or otherwise "folded" DNA structures. Colorimetric assays employing this mechanism for the detection of hybridization are sensitive and convenient—picomolar concentrations of target DNA are readily detected with the naked eye, and the sensor works even when challenged with complex sample matrices such as blood serum. Likewise, by employing the binding-induced folding or association of aptamers we have generalized the approach to the specific and convenient detection of proteins, small molecules, and inorganic ions. Finally, this new biosensor approach is quite straightforward and can be completed in minutes without significant equipment or training overhead.

biosensor | aptamer | visual detection | thrombin detection | cocaine detection

Gold nanoparticle colorimetric biosensors have seen significant applications in diagnostics, environmental monitoring, and antibioterrorism supporting unaided, visual readout (1–12). Commonly, the relevant nanoparticles are covalently modified with either a probe DNA or an aptamer such that hybridization (13–16) or aptamer-target interactions (17–27), for example the scanometric method developed by Mirkin (25), which is a very sensitive and specific tool, crosslink them, inducing aggregation. The second broad approach utilizes unmodified nanoparticles. (28–30) These two approaches, however, suffer from time-consuming (20–40 h of assembly) and relatively poor (low nanomolar) detection limits, respectively. Here, a unique, colorimetric sensing strategy employing a simple but selective combination of a single-stranded DNA probe, a positively charged, water-soluble conjugated polyelectrolyte, and unmodified gold nanoparticles is demonstrated. The universality of this method allows detection of a broad range of targets, including nucleic acid (DNA) sequences, proteins, small molecules, and inorganic ions. Our approach is rapid (turnaround time is 5–10 min) and sensitive (picomolar concentrations of target DNA are readily detected with the naked eye, even in complex sample matrices like blood serum). Hence, an operator with minimum scientific overhead can easily employ this technique.

Generally, the gold nanoparticle applications typically rely on a quantitative coupling between target recognition and the aggregation of the nanoparticles, which, in turn, leads to a dramatic change in the photonic properties—and thus the color—of the nanoparticle solution. This colorimetric "readout" avoids the relative complexity inherent in optical imaging/detection methodologies and thus may prove suitable for point-of-care and developing world applications (9–12). Examples for the covalently modified nanoparticles include the work of Mirkin and collaborators, who pioneered the use of gold nanoparticle-DNA conjugates (22, 23) for the sensitive detection of DNA and proteins (24–27). For the unmodified nanoparticles, Li and Rothberg have shown that, at high ionic strength, single-stranded—but not double-stranded—DNA protects unmodified gold nanoparticles from aggregating, thus modifying their color (28–30). Employing this mechanism, these authors have demonstrated a colorimetric assay for specific DNA sequences.

Our approach to the application of gold nanoparticles in optical biosensing relies on the recent observations that (i) both single-stranded DNA and double-stranded DNA prevent aggregation of gold nanoparticles at low salt concentrations (28–30); (ii) conjugated polyelectrolytes lead to the ready aggregation of such nanoparticles (31), and (iii) previous work has demonstrated that, at certain conditions, the cationic conjugated polyelectrolyte poly [(9,9-bis (6'-N,N,N-trimethylammonium) hexyl) fluorene-alt-1,4-phenylene] bromide (PFP-Br) binds single-stranded DNA preferentially to double-stranded or otherwise "folded" DNA, (32–34). This appears to arise due to the greater hydrophobicity of single-stranded DNA. Upon reducing the strength of the hydrophobic interactions, the electrostatic attraction becomes the important interaction that regulates the binding between the water-soluble conjugated polymer and DNA (33). The different affinities between the cationic conjugated polymer and various forms of DNA (single-stranded DNA and double-stranded DNA and single-stranded DNA and complex DNA folds) can be used to design a variety of biosensors (32–34).

## Results

Inspired by the above, we have developed a unique colorimetric assay for the detection of nucleic acids, small-molecules, proteins, and inorganic ions that relies on unmodified gold nanoparticles but that employs the conjugated, positively charged, water-soluble polymer poly [(9,9-bis (6'-N,N,N-trimethylammonium) hexyl) fluorene-alt-1,4-phenylene] bromide). We have employed cationic conjugated polyelectrolytes to efficiently sequester single-stranded—but not double-stranded or otherwise "folded"—DNA from nanoparticles, leading to their aggregation and color change (Fig. S1) (32–34). We have then used this effect as the
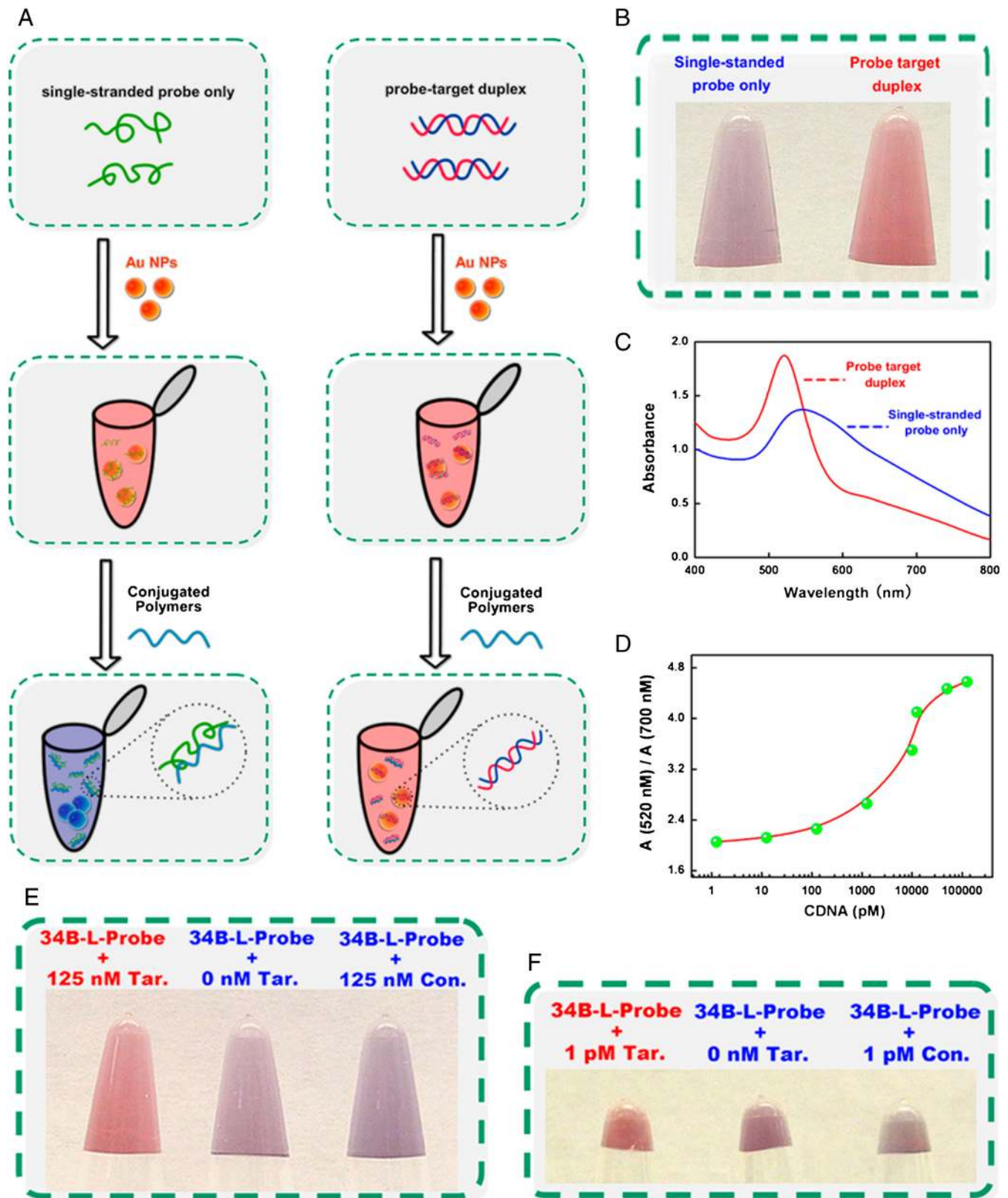
APPLIED BIOLOGICAL SCIENCES

**Fig. 1.** Here we demonstrate a sensitive colorimetric assay for the detection of DNA. We find that, whereas a mixture of a positively charged, water-soluble, conjugated polyelectrolyte and single-stranded DNA leads to the aggregation of gold nanoparticles (and, consequently, a readily detectable change in their color), admixtures of this polymer with double-stranded DNA does not similarly produce a color change. (*A*) Here we have used this effect as the basis of a ready colorimetric assay for the detection of specific oligonucleotides. The assay is rapid and sensitive: (<125 attomoles of target in 10 μL solution differentiates a color change observable with the naked eye in less than 10 min. (*B*) According to the scheme, the solution only contains a single-stranded probe that makes the gold nanoparticles aggregate (blue), while the probe–target duplex keeps the gold nanoparticles stable (red). (*C*) The ratio $A_{520}/A_{700}$ for a perfect match target is much larger than no target indicating the specificity of our assay. (*D*) By calculating the ratio $A_{520}/A_{700}$ form the UV-Vis test we could measure the target concentration, which is also crucial for detection. Shown is our ability to specifically detect target DNA molecules at both *E*, high (125 nM), and *F*, (1.25 pM) concentrations.

basis for an assay for the sensitive, colorimetric detection of a wide range of molecular analytes.

For the detection of DNA (Fig. 1A), we first prepare a control sample containing a single-stranded probe DNA and a test sample containing the probe DNA and its complementary DNA target. A solution of 20 nm gold nanoparticles is added to both, producing a readily apparent red color due to the intense surface plasmon resonance (SPR) absorption of the nanoparticles at 520 nm. The subsequent addition of the conjugated polyelectro-lyte sequesters most of single-stranded DNA, leaving it unable to stabilize the nanoparticles against aggregation and thus leading to a characteristic blue color for the control sample (which only contains single-stranded DNA). In the presence of the complementary target sequence a significant concentration of double-stranded DNA is formed, which only weakly binds the conjugated polyelec-trolytes and thus remains largely free to stabilize the nanoparticles against aggregation. This, in turn, causes the sample to retain the red color associated with dispersed nanoparticles (Fig. 1B).
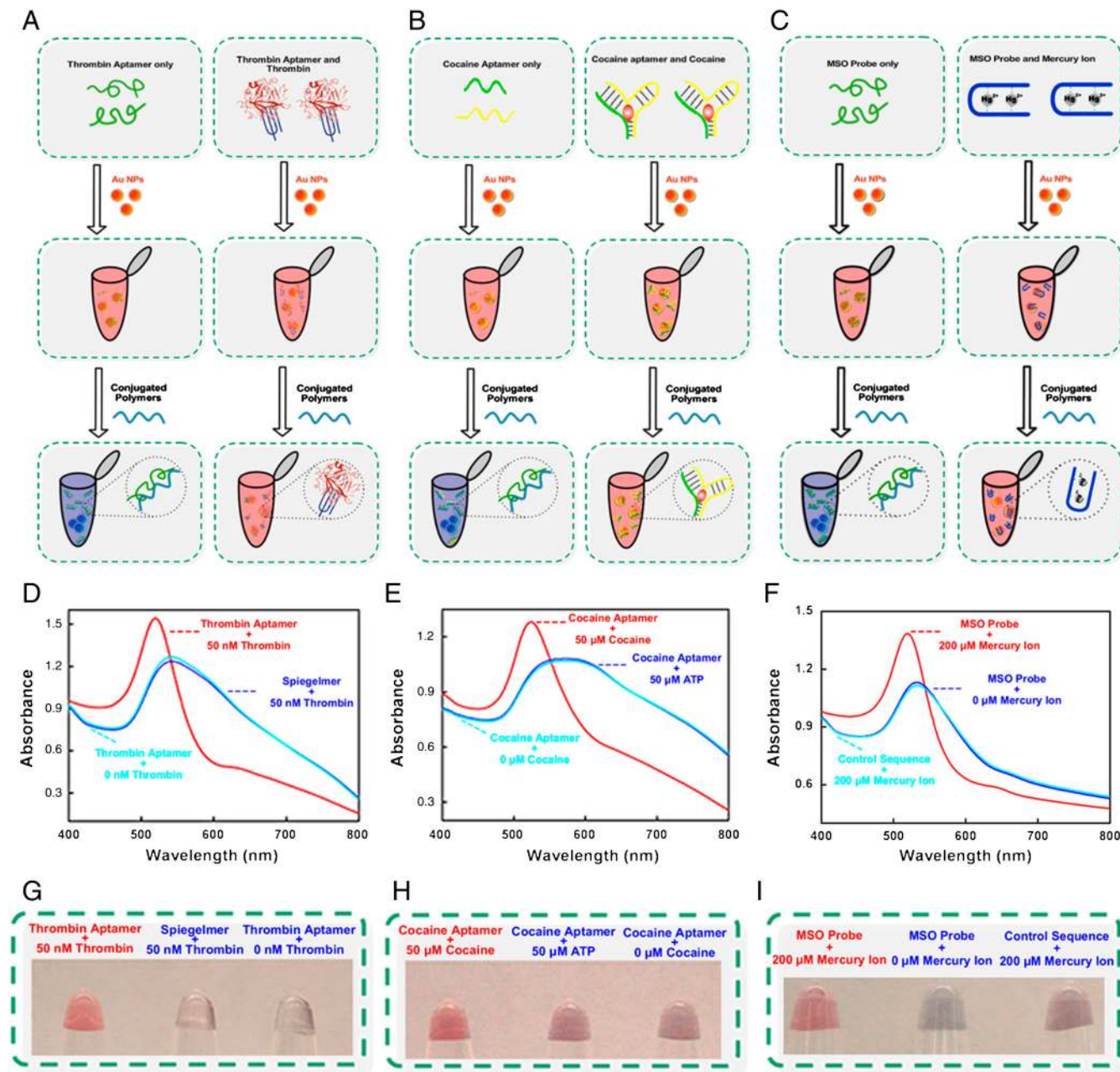


**Fig. 2.** Our assay also could easily be expanded to the detection of proteins, small molecules, and ions. (A) A thrombin aptamer has been used in our protein detection. (B) We use a sandwich approach based on single aptamer sequences in our cocaine detection. (C) We use a mercury-responsive sequence that folds in the presence of Hg (II) to detect the Hg (II). (D) When the sample contains thrombin, it folded the aptamer into G-quadruplex structure together, which stabilized the gold nanoparticles remaining red. The sample containing control probe or no target induced the aggregation, which shifts the absorption from 520 nM to the longer wavelength, resulting in the characteristic red-blue color change. The detect limit for thrombin is 10 nM. (E) When the sample contains cocaine, it associate two part aptamer together, which stabilize the gold nanoparticles remaining red. The sample containing ATP or no target induced the aggregation, which shifts the absorption from 520 nM to the longer wavelength, resulting in the characteristic red-blue color change. The detect limit for cocaine is 10 μM. (F) The sample containing no target induced the aggregation, which shifts the absorption from 520 nM to the longer wavelength, resulting in the characteristic red-blue color change. The detect limit for Hg (II) is 50 μM. (G, H, and I) This color change allows us to easily differentiate between target-containing and target-free samples by visual inspection.

The color change associated with the lack of double-stranded DNA allows us to easily differentiate the single-stranded DNA probe and the double-stranded probe-target duplex via visual inspection at concentrations as low as 1.25 pM (Fig. 1 E and F), a detection limit comparable to those of many previously reported fluorescent DNA assays and enzyme-linked amplified assays (35). A more quantitative analysis can be made using UV-Vis spectroscopy. Specifically, the absorbance of the solution at 520 nm increases and the absorbance at 700 nm decreases when the concentration of double-stranded DNA is increased from 1.25 pM to 125 nM (Fig. 1 C and D). A series of control experiments confirm the specificity of the assay: As expected, duplexes between the 34-base pair probe and targets containing 3-, 5- or 7 base-pair mismatches do not stabilize the nanoparticles against aggregation, leading to the characteristic blue color (Fig. S2).

A key feature of our method is that, unlike approaches that utilize functionalized nanoparticles, hybridization and binding occur under conditions that can be independently regulated and optimized. For example, our approach relies on an ability to detect double-stranded probe–target duplexes. Thus, a potential disturbance is that any double-stranded DNA contaminating the sample will also stabilize the nanoparticles. Because we can optimize test conditions, the pretreatment of the sample with Exonuclease III, which provides a ready and convenient solution degrading any double-stranded DNA initially present in the sample (Fig. S3). Thus our assay can be made quite specific. Likewise the assay is selective and performs well even when challenged directly in complex biological media, such as target-doped blood serum (Fig. S4).

## Discussion

While the detection of DNA is of significant clinical utility in its own right, by employing aptamers, nucleic acid molecules that have been selected in vitro to bind to specific molecular targets (36–39), our colorimetric assay can also be expanded to the detection of nonnucleic acid targets. Specifically, because it is relatively easy to reengineer aptamers such that they undergo a transition from largely single-stranded to a folded, compact structure upon target binding (40–44), and because the conjugated polyelectrolyte only weakly binds with these compact, folded structures (31–34), we can adapt our assay to the detection of the aptamer's binding partner (Fig. 2).

As a first example of the broader applicability of our approach, we developed an assay for the small molecule cocaine using the anticocaine aptamer of Stojanovic (39–42). To do so we modified the aptamer sequence slightly (see *Methods*) to prevent interstrand binding and then cut the sequence into two short, single-stranded pieces (40, 41). We then prepared two samples: a control sample containing only these fragments and a test sample containing the two aptamer fragments and cocaine. Upon adding a solution of ~20 nm gold nanoparticles, both samples turn red

due to the intense surface plasmon resonance absorption of the nanoparticles. Upon the addition of the conjugated polyelectrolyte, the nanoparticles in the control solution aggregate and the solution turns blue. The test sample, in contrast, retains its red color, presumably because cocaine binding drives the two pieces to associate (40–42) to form a well-folded, largely double-stranded aptamer that only weakly binds with the conjugated polyelectrolytes and thus remains free to inhibit nanoparticle aggregation (Fig. 2). This color change supports the ready detection of cocaine via visual inspection. As expected, this sensor does not respond when challenged with other small molecules, such as ATP (Fig. 2).

Abundant literature suggests that it is relatively easy to modify aptamers such that they only fold upon target binding (40–45), an effect that also supports our assay. As examples we have used Bock's thrombin-binding aptamer, which folds from a single-stranded state to a largely G-quadruplex structure upon target binding (43, 44) and a mercury-responsive sequence that folds in the presence of Hg (II) (45–49). Once again, we employ control (aptamer-only) and test (aptamer-plus-target) solutions, which, upon mixing with ~20 nm gold nanoparticles, produce the characteristic absorption at 520 nm. In the absence of target, both aptamers are single-stranded and thus do not stabilize the gold nanoparticles against aggregation in the presence of the polymer. Upon target binding, however, the aptamers fold, reducing their interactions with the conjugated polyelectrolytes and allowing them to prevent nanoparticle aggregation (Fig. 2). The resultant color change supports the easy differentiation between target-containing and target-free samples via visual inspection.

The strategy described in this report offers advantages over many existing sensing methodologies. First, our approach is likely universal; here, for example, we have shown that it is applicable to the detection of nucleic acids, small molecules, proteins, and inorganic ions. Second, our approach is convenient, requiring only the mixing of several solutions at room temperature to achieve rapid, semiquantitative detection via visual inspection or quantitative detection via visible light absorbance spectroscopy. Third, the detection of DNA using this approach is sensitive. We achieve, for example, low picomolar sensitivity for DNA detection, comparing very favorably with previously reported methods (Table 1) (28, 35, 50–52). Fourth, each step in the process (pretreatment with Exonuclease, the binding of the target to the DNA probe, the addition of conjugated polyelectrolytes) is performed separately, allowing each step to be optimized independently. Finally, the detection process is rapid and convenient.

## Methods

In a typical gold nanoparticles/CP assay, the DNA probes were dissolved in a salt solution (112.5 mM NaCl) to form 1.25 µM probe solution at room temperature. Such solution (2.5 µL) was added to gold nanoparticles solution (25 µL), and the obtained solution was incubated for 1 min at room temperature. The concentrations of probes are 125 nM in this solution unless specially indicated. After that CP (5 µL, 1 µM) was added to the above solution,

**Table 1. Comparison of sensors for DNA detection**

| Detection method | Strategy | Detection limit | Existing problems |
|---|---|---|---|
| Colorimetric (this work) | AuNP & conjugated polyelectrolyte | 1 pM (naked eyes) | Not applicable for colored samples |
| Colorimetric (28) | AuNP & salt | 4.3 nM (naked eyes) | Detect limit not applicable for colored samples |
| Colorimetric (50) | Enzyme amplification magnetic separation | 100 pM (naked eyes) | Multistep process, cumbersome preparation of functionalized gold nanoparticles and magnetic bead. Time-consuming (>1 day), not applicable for colored samples |
| Electrochemistry (51) | Electron transfer | 10 pM | Dual-labeled oligos. Time-consuming (≈5 hours) |
| Electrochemistry (52) | Enzyme Amplification & PNA Probe & AgNP | 10 fM | Multistep process, stability of enzyme, dual label of DNA, reagent intensive. Time-consuming (≈5 hours) |
| Fluorescence (35) | Conjugated Polyelectrolyte FRET | 2.14 pM | Using expensive and complicated instruments for detection. Time-consuming (≈3 hours) |

followed by either visual observation or UV/Vis characterization. The total volume of the final solutions in this work may differ, but the volume ratio of the above DNA, gold nanoparticles solution, and CPs is 1 : 10 : 2. In cocaine assays, the 3′ fragment and 5′ fragment were dissolved in salt solution (112.5 mM NaCl) to form 0.625 uM 3′ fragment and 0.625 uM 5′ fragment probe solution at room temperature. Then cocaine was added to the above solution. This solution (2.5 μL) was added to gold nanoparticles solution (25 μL), and the obtained solution was incubated for 2 min at room temperature. After that CP (5 μL, 1 μM) was added, followed by either visual observation or UV/Vis characterization. For the thrombin assay, the thrombin aptamer (or spiegelmer) was dissolved in a salt solution (112.5 mM NaCl)

to form 1.25 μM probe solution at room temperature. Then thrombin was added followed by incubation for 20 min. After that CP (5 μL, 1 μM) was added, followed by either visual observation or UV/Vis characterization.

1. Thompson DG, Enright A, Faulds K, Smith WE, Graham D (2008) Ultrasensitive DNA detection using oligonucleotide-silver nanoparticle conjugates. *Anal Chem* 80(8):2805–2810.
2. Cho M, Han MS, Ban C (2008) Detection of mismatched DNAs via the binding affinity of MutS using a gold nanoparticle-based competitive colorimetric method. *Chem Commun*(38):4573–4575.
3. Béra-Abérem M, Ho H-A, Leclerc M (2004) Functional polythophenes as optical chemo- and biosensors. *Tetrahedron* 60(49):11169–11173.
4. Reynolds RA, Mirkin CA, Letsinger RL (2000) Homogeneous, nanoparticle-based quantitative colorimetric detection of oligonucleotides. *J Am Chem Soc* 122(15):3795–3796.
5. Ho H-A, et al. (2002) Colorimetric and fluorometric detection of nucleic acids using cationic polythiophene derivatives. *Angew Chem Int Edit* 41(9):1548–1551.
6. Storhoff JJ, Mirkin CA (1999) Programmed materials synthesis with DNA. *Chem Rev* 99(7):1849–1862.
7. Kim S, et al. (2009) Bioinspired colorimetric detection of calcium(II) ions in serum using calsequestrin-functionalized gold nanoparticles. *Angew Chem Int Edit* 48(23):4138–4141.
8. Peter K, Nilsson R, Inganäs O (2003) Chip and solution detection of DNA hybridization using a luminescent zwitterionic polythiophere derivative. *Nat Mater* 2(6):419–424.
9. Liu JW, Cao ZH, Lu Y (2009) Functional nucleic acid sensors. *Chem Rev* 109(5):1948–1998.
10. Ahn DJ, Lee S, Kim JM (2009) Rational design of conjugated polymer supramolecules with tunable colorimetric responses. *Adv Funct Mater* 19(10):1483–1496.
11. Ali MM, Li YF (2009) Colorimetric sensing by using allosteric-DNAzyme-coupled rolling circle amplification and a peptide nucleic acid-organic dye probe. *Angew Chem Int Edit* 48(19):3512–3515.
12. Pu KY, Liu B (2009) Intercalating dye harnessed cationic conjugated polymer for real-time naked-eye recognition of double-stranded DNA in serum. *Adv Funct Mater* 19(9):1371–1378.
13. Elghanian R, Storhoff JJ, Mucic RC, Letsinger RL, Mirkin CA (1997) Selective colorimetric detection of polynucleotides based on the distance-dependent optical properties of gold nanoparticles. *Science* 277(5329):1078–1081.
14. Storhoff JJ, Elghanian R, Mucic RC, Mirkin CA, Letsinger RL (1998) One-pot colorimetric differentiation of polynucleotides with single base imperfections using gold nanoparticle probes. *J Am Chem Soc* 120(9):1959–1964.
15. Demers LM, et al. (2000) A fluorescence-based method for determining the surface coverage and hybridization efficiency of thiol-capped oligonucleotides bound to gold thin films and nanoparticles. *Anal Chem* 72(22):5535–5541.
16. Storhoff JJ, et al. (2000) What controls the optical properties of DNA-linked gold nanoparticle assemblies?. *J Am Chem Soc* 122(19):4640–4650.
17. Liu J, Lu Y (2005) Stimuli-responsive disassembly of nanoparticle aggregates for light-up colorimetric sensing. *J Am Chem Soc* 127(36):12677–12683.
18. Liu JW, Lu Y (2004) Optimization of a Pb2+ -directed gold nanoparticle/DNAzyme assembly and its application as a colorimetric biosensor for Pb2+. *Chem Mater* 16(17):3231–3238.
19. Liu JW, Lu Y (2004) Accelerated color change of gold nanoparticles assembled by DNAzymes for simple and fast colorimetric Pb2+ detection. *J Am Chem Soc* 126(39):12298–12305.
20. Liu JW, Lu Y (2004) Adenosine-dependent assembly of aptazyme-functionalized gold nanoparticles and its application as a colorimetric biosensor. *Anal Chem* 76(6):1627–1632.
21. Liu JW, Lu Y (2006) Fast colorimetric sensing of adenosine and cocaine based on a general sensor design involving aptamers and nanoparticles. *Angew Chem Int Edit* 45(1):90–94.
22. Mirkin CA, Letsinger RL, Mucic RC, Storhoff JJ (1996) A DNA-based method for rationally assembling nanoparticles into macroscopic materials. *Nature* 382(6592):607–609.
23. Rosi NL, Mirkin CA (2005) Nanostructures in biodiagnostics. *Chem Rev* 105(4):1547–1562.
24. Cao YWC, Jin RC, Mirkin CA (2002) Nanoparticles with Raman spectroscopic fingerprints for DNA and RNA detection. *Science* 297(5586):1536–1540.
25. Taton TA, Mirkin CA, Letsinger RL (2000) Scanometric DNA array detection with nanoparticle probes. *Science* 289(5485):1757–1760.
26. Zhang J, Song SP, Wang LH, Pan D, Fan C (2007) A gold nanoparticle-based chrono-coulometric DNA sensor for amplified detection of DNA. *Nat Protoc* 2(11):2888–2895.
27. McKenzie F, Faulds K, Graham D (2007) Sequence-specific DNA detection using high-affinity LNA-functionalized gold nanoparticles. *Small* 3(11):1866–1868.

28. Li HX, Rothberg L (2004) Colorimetric detection of DNA sequences based on electrostatic interactions with unmodified gold nanoparticles. *Proc Natl Acad Sci USA* 101(39):14036–14039.
29. Li HX, Rothberg LJ (2004) Label-free colorimetric detection of specific sequences in genomic DNA amplified by the polymerase chain reaction. *J Am Chem Soc* 126(35):10958–10961.
30. Wang LH, Liu XF, Hu XF, Song SP, Fan CF (2006) Unmodified gold nanoparticles as a colorimetric probe for potassium DNA aptamers. *Chem Commun*(36):3780–3782.
31. Polavarapu L, Xu QH (2008) Water-soluble conjugated polymer-induced self-assembly of gold nanoparticles and its application to SERS. *Langmuir* 24(19):10608–10611.
32. Liu B, Bazan GC (2004) Homogeneous fluorescence-based DNA detection with water-soluble conjugated polymers. *Chem Mater* 16(23):4467–4476.
33. Xia F, et al. (2010) On the binding of cationic, water-soluble conjugated polyelectrolytes to DNA: Electrostatic and hydrophobic interactions. *J Am Chem Soc* 132(4):1252–1254.
34. Wang S, Liu B, Gaylord & Bazan GC Size-specific interactions between single- and double-stranded oligonucleotides and cationic water-soluble oligofluorenes. *Adv Funct Mater* 13(6):463–467.
35. He F, et al. (2008) Selective and homogeneous fluorescent DNA detection by target-induced strand displacement using cationic conjugated polyelectrolytes. *Anal Chem* 80(6):2239–2243.
36. Willner I, Zayats M (2007) Electronic aptamer-based sensors. *Angew Chem Int Edit* 46(34):6408–6418.
37. You KM, Lee SH, Im A, Lee SB (2003) Aptamers as functional nucleic acids: In vitro selection and biotechnological applications (Translated from English). *Biotechnol Bioproc E* 8(2):64–75 (in English).
38. Luzi E, Minunni M, Tombelli S, Mascini M (2003) New trends in affinity sensing: aptamers for ligand binding. *Trac-Trend Anal Chem* 22(11):810–818.
39. Stojanovic MN, de Prada P, Landry DW (2001) Aptamer-based folding fluorescent sensor for cocaine. *J Am Chem Soc* 123(21):4928–4931.
40. Zuo XL, Xiao Y, Plaxco KW (2009) High specificity, electrochemical sandwich assays based on single aptamer sequences and suitable for the direct detection of small-molecule targets in blood and other complex matrices. *J Am Chem Soc* 131(20):6944–6945.
41. Zhang J, et al. (2008) Visual cocaine detection with gold nanoparticles and rationally engineered aptamer structures. *Small* 4(8):1196–1200.
42. Freeman R, Sharon E, Tel-Vered R, Willner I (2009) Supramolecular cocaine-aptamer complexes activate biocatalytic cascades. *J Am Chem Soc* 131(14):5028–5029.
43. Bock LC, Griffin LC, Latham JA, Vermaas EH, Toole JJ (1992) Selection of single-stranded-DNA molecules that bind and inhibit human thrombin. *Nature* 355(6360):564–566.
44. Xiao Y, Lubin AA, Heeger AJ, Plaxco KW (2005) Label-free electronic detection of thrombin in blood serum by using an aptamer-based sensor. *Angew Chem Int Edit* 44(34):5456–5459.
45. Hollenstein M, Hipolito C, Lam C, Dietrich D, Perrin DM (2008) A highly selective DNAzyme sensor for mercuric ions. *Angew Chem Int Edit* 47(23):4346–4350.
46. Li D, Wieckowska A, Willner I (2008) Optical analysis of Hg2+ ions by oligonucleotide-nanoparticle hybrids and DNA-based machines. *Angew Chem Int Edit* 47(21):3927–3931.
47. Song FL, Watanabe S, Floreancig PE, Koide K (2008) Oxidation-resistant fluorogenic probe for mercury based on alkyne oxymercuration. *J Am Chem Soc* 130(49):16460–16461.
48. Nolan EM, Lippard SJ (2008) Tools and tactics for the optical detection of mercuric ion. *Chem Rev* 108(9):3443–3480.
49. Wang LH, et al. (2008) Gold nanoparticle-based optical probes for target-responsive DNA structures. *Gold Bull* 41(1):37–41.
50. Li J, et al. (2008) Enzyme-based multi-component optical nanoprobes for sequence-specific detection of DNA hybridization. *Adv Mater* 20(3):497–500.
51. Fan CH, Plaxco KW, Heeger AJ (2003) Electrochemical interrogation of conformational changes as a reagentless method for the sequence-specific detection of DNA. *Proc Natl Acad Sci USA* 100(16):9134–9137.
52. Zhang J, Ting BP, Jana NR, Gao ZQ, Ying JY (2009) Ultrasensitive electrochemical DNA biosensors based on the detection of a highly characteristic solid-state process. *Small* 5(12):1414–1417.

APPLIED BIOLOGICAL SCIENCES

# Supporting Information

## Xia et al. 10.1073/pnas.1005632107

### SI Text

**Mechanism Discussion.** The mechanism underlying this detection method appears to be linked to the different affinities with which double- and single-stranded DNA bind to the conjugated polymer (1–3). Because of this difference, the polymer does not bind all double-stranded DNA to prevent aggregation but efficiently removes single-stranded DNA from the gold nanoparticles, which, in turn, allows the nanoparticles to aggregate and change color. In support of this argument, dye-modified single-stranded DNA is quenched far more effectively by conjugated polyelectrolytes than is the equivalent dye-modified double-stranded DNA (Fig. S1 *A* and *B*), indicating that the polymer binds to single-stranded DNA binds more tightly than it binds double-stranded DNA. Although the single-stranded DNA has less charge density than double-stranded DNA, the additional hydrophobic interactions in ssDNA may compensate for the weaker electrostatic interactions due to its flexible structure and more exposed hydrophobic region (1–6).

**Test of Bio-Specificity.** A series of control experiments confirm the specificity of the assay. As expected, duplexes between the 34-base pair probe and targets containing 3-, 5 or 7 base-pair mismatches (Fig. S2) produce the same blue color as control samples lacking any target.

**Optimizing the Conditions.** The color change, induced by bio-specific binding to the unmodified gold nanoparticles, occurs under predetermined and separately optimized conditions. For example, our approach relies on the ability to detect double-stranded probe-target duplexes. A potential disturbance is thus that any double-stranded DNA contaminating the sample will stabilize the nanoparticles. However we could optimize test conditions, the pretreatment of the sample with Exonuclease III provides a ready and convenient solution to this problem. Specifically, this enzyme catalyzes the removal of mononucleotides from the 3′-end of double-stranded DNA but does not degrade single-stranded DNA. For example, an actual sample could contain some kind of double-stranded DNA (here, 27 bases double-stranded DNA). If so, when the sample contains no perfect DNA (here, 7-mismatch-DNA) to the probe, the double-stranded DNA could stabilize AuNPs using the above described assay (Fig. S4*A*). If, however, we first treat the sample with Exonuclease III followed by heat deactivation of the enzyme (via immersion for 5 min in a 65 °C water bath), the problem is solved without disrupting the method's ability to detect the authentic target (Fig. S3 *B*, *C*, and *D*).

**Recognition of dsDNA in Serum.** To demonstrate that the new assay is able to recognize dsDNA in biological media, we prepared the ssDNA and dsDNA ample in 56 mM NaCl solution containing 30 vol% serum. Serum is plasma without fibrinogen or other clotting factors; serum contains proteins, glucose, mineral ions, hormones, and other biological substances. We added the above solution into the AuNPs and followed added CP. The final concentration for the serum is 3 vol%. And both of the solutions are red at this stage. Then we centrifuged the two samples for 2 min at 14,100 rcf. Finally the sample contains dsDNA retains red, while the sample with ssDNA turns to very light blue (Fig. S4).

**Details of the Assay.** Tables S1, S2, S3, and S4 show the details of the assay.

**Materials.** Gold nanoparticles (20 nm) were obtained from Sigma-Aldrich. The AuNP solution was centrifuged to a concentrated solution; the optimum conditions were centrifuging for 15 min at 4 °C, with a RCF of 16100 g. Exonuclease III was obtained from Sigma-Aldrich. DNase I (RNase-free) was obtained from New England Biolabs. Human R-thrombin was obtained from Haematologic Technologies Inc.; Essex Junction, VT. Cocaine, mercury ion and serum were used as received. The sequences of the involved oligonucleotides, which were all purchased from Biosearch Technologies, Inc., are listed in following. UV/Vis absorption spectroscopy was performed with a Beckman Coulter DU 800 spectrophotometer and photographs were taken with a Nikon digital camera. The Polymer, poly[(9,9-bis(6′-N,N,N-trimethylammonium)hexyl)fluorene-alt-1,4-phenylene] bromide (PFP-Br) was prepared according to the published references (7, 8).

***The sequences of the DNA probes and targets used in this work.*** *34-mer-Linear-Probe*: 5′-TGGATCGGCGTTTTATTCTTGTTCA-GATATTCAA-3′

   *34-mer-Linear-Target 0 mismatch*: 5′-TTGAATATCTGAACA-AGAATAAAACGCCGATCCA-3′

   *34-mer-Linear-Target 3 mismatch*: 5′-TTGAATATCTGAACA-A**CTT**TAAAACGCCGATCCA-3′

   *34-mer-Linear-Target 5 mismatch*: 5′-TTGAATATCTGAACA-**TCTTA**AAAACGCCGATCCA-3′

   *34-mer–Linear-Target 7 mismatch*: 5′-TTGAATATCTGAAC-**TTCTTAT**AAACGCCGATCCA-3′

   *27-mer–Linear-Probe*: 5′-GACACTGGATCGGCGTTTTATT-CACAG-3′

   *27-mer–Linear-Target 0 mismatch*: 5′-CTGTGAATAAAACG-CCGATCCAGTGTC-3′

   *27-mer–Linear-Target 7 mismatch*: 5′-CTGTGAATAA**TTGCG-GC**ATCCAGTGTC-3′

   *3 fragment for anticocaine aptamer*: 5′-AGACAAGGAAAA-3′
   *5 fragment for anticocaine aptamer*: 5′-TCCTTCAATGAAG-TGGGTCG-3′

   *Thrombin Aptamer*: 5′-TAAGTTCATCTCCCCGGTTGGTG-TGGTTGGT-3′

   *Spiegelmer*: 5′-TAAGTTCATCTCCCCGGTTGGTGTGGTT-GGT-3′

   *Mercury-Specific Oligonucleotide (MSO) probe*: 5′-TGTTTCTT-TCTTCCCCTTGTTTGTTTCA-3′

   *Mercury-Control sequence*: 5′-TAGCTATGGAATTCCTCG-TAGGCA-3′

1. Wang S, Liu B, Gaylord BS & Bazan GC (2003) Size-specific interactions between single- and double-stranded oligonucleotides and cationic water-soluble oligofluorenes *Adv Funct Mater* 13(6):463–467.
2. Liu B, Bazan, GC (2004) Homogeneous fluorescence-based DNA detection with water-soluble conjugated polymers. *Chem Mater* 16(23):4467–4476.
3. Xia F et al. (2010) On the binding of cationic, water-soluble conjugated polyelectrolytes to DNA: Electrostatic and hydrophobic interactions. *J Am Chem Soc* 132 (4): 1252–1254.
4. Liu B, Gaylord BS, Wang S, & Bazan GC (2003) Effect of chromophore-charge distance on the energy transfer properties of water-soluble conjugated oligomers. *J Am Chem Soc* 125(22):6705–6714.
5. Gaylord BS, Heeger AJ, Bazan GC (2003) DNA hybridization detection with water-soluble conjugated polymers and chromophore-labeled single-stranded DNA. *J Am Chem Soc* 125(4):896–900.
6. Xu Q-H et al. (2004) Time-resolved energy transfer in DNA sequence detection using water-soluble conjugated polymers: The role of electrostatic and hydrophobic interactions. *Proc Natl Acad Sci USA* 101(32):11634–11639.

7. Yang RQ, Wu HB, Cao Y, Bazan GC (2006) Control of cationic conjugated polymer performance in light emitting diodes by choice of counterion. *J Am Chem* 128(45): 1422–14423.

8. Hoven C et al. (2007) Ion motion in conjugated polyelectrolyte electron transporting layers. *J Am Chem Soc* 129(36):10976–10977.
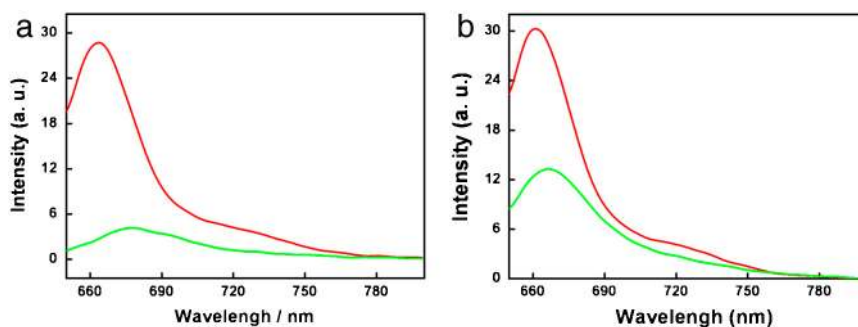
**Fig. S1.** Experiments for preferential affinity between ssDNA with PFP-Br. (*A*) Fluorescence emitted from Cy5 attached to 34-mer-DNA probe (red curve) and after adding PFP-Br (green curve). (*B*) Fluorescence emitted from Cy5 attached to 34-mer-DNA probe with target DNA (red curve) and after adding PFP-Br (green curve).
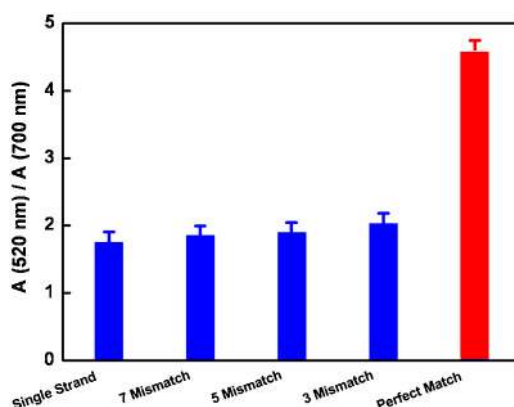


**Fig. S2.** The absorbance ratio ($A_{520}/A_{700}$) versus each corresponding DNA/AuNPs/CPs solution.
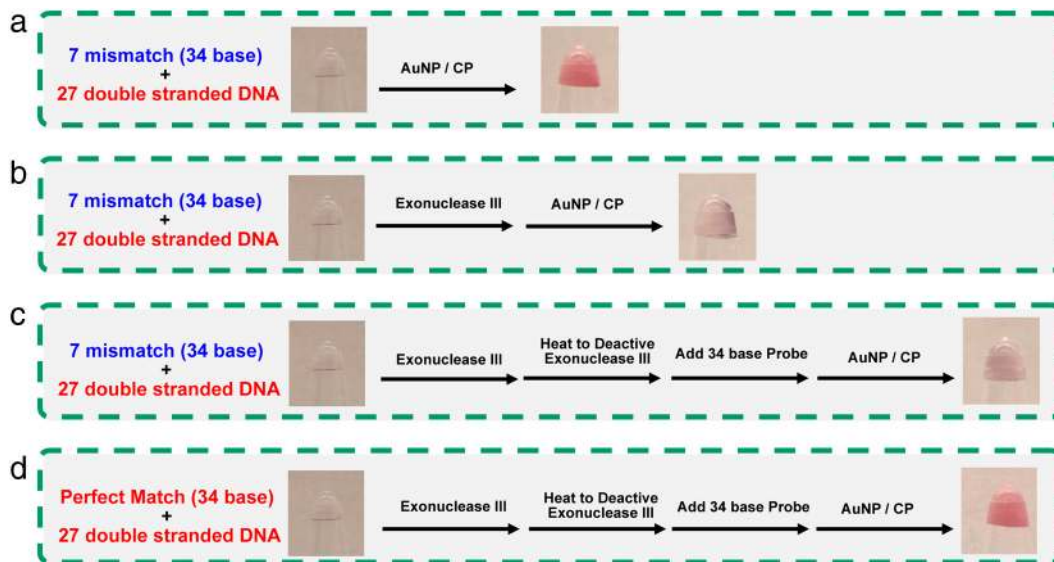


**Fig. S3.** Optimizing the conditions in the DNA Test via pretreatment with Exonuclease III. (*A*) A test sample containing a contaminating double-stranded DNA adopts the characteristic red color associated with the presence of no-authentic sample. (*B*) If the sample is pretreated with Exonuclease III this sample could not stabilize AuNPs (see *C*). (*D*) Finally, a sample containing both contaminating double-stranded DNA and authentic, single-stranded target provides a correct, positive response after this treatment protocol.
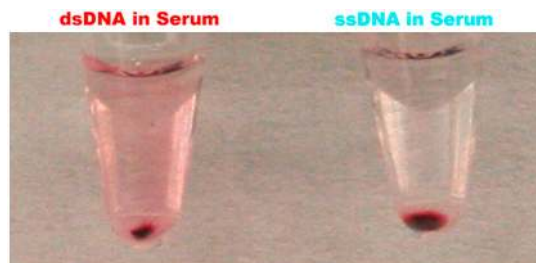
**Fig. S4.** Colorimetric detection of oligonucleotide hybridization in serum. 34-mer-linear-probes detect the target (dsDNA) and control (ssDNA).

## Table S1. The assay of 34 base probe

| | Step 1. Solution 1 | | | | |
|---|---|---|---|---|---|
| | 34 base DNA Probe | 34 base DNA Probe+34 base DNA target (perfect match to probe) | 34 base DNA Probe+34 base DNA control (3 mismatch to probe) | 34 base DNA Probe+34 base DNA control (5 mismatch to probe) | 34 base DNA Probe+34 base DNA control (7 mismatch to probe) |
| Color | Colorless | Colorless | Colorless | Colorless | Colorless |
| | Step 2. Adding solution 1 to AuNPs solutions to make solution 2 | | | | |
| | 34 base DNA Probe+AuNPs | 34 base DNA Probe+34 base DNA target (perfect match to probe)+AuNPs | 34 base DNA Probe+34 base DNA control (3 mismatch to probe)+AuNPs | 34 base DNA Probe+34 base DNA control (5 mismatch to probe)+AuNPs | 34 base DNA Probe+34 base DNA control (7 mismatch to probe)+AuNPs |
| Color | Red | Red | Red | Red | Red |
| | Step 3. Adding conjugated polyelectrolyte (CP) into solution 2 | | | | |
| | 34 base DNA Probe+AuNPs +CP | 34 base DNA Probe+34 base DNA target (perfect match to probe)+AuNPs+CP | 34 base DNA Probe+34 base DNA control (3 mismatch to probe)+AuNPs+CP | 34 base DNA Probe+34 base DNA control (5 mismatch to probe)+AuNPs+CP | 34 base DNA Probe+34 base DNA control (7 mismatch to probe)+AuNPs+CP |
| Color | Blue Probe | Red Probe+Target | Blue Probe+Control | Blue Probe+Control | Blue Probe+Control |

## Table S2. The assay for cocaine aptamer

| | Step 1. Solution 1 | | |
|---|---|---|---|
| | Cocaine aptamer 3′ fragment and 5′ fragment | Cocaine aptamer 3′ fragment and 5′ fragment+Cocaine | Cocaine aptamer 3′ fragment and 5′ fragment+ATP |
| Color | Colorless | Colorless | Colorless |
| | Step 2. Adding solution 1 to AuNPs solutions to make solution 2 | | |
| | Cocaine aptamer 3′ fragment and 5′ fragment+AuNPs | Cocaine aptamer 3′ fragment and 5′ fragment+Cocaine+AuNPs | Cocaine aptamer 3′ fragment and 5′ fragment+ATP +AuNPs |
| Color | Red | Red | Red |
| | Step 3. Adding conjugated polyelectrolyte (CP) into solution 2 | | |
| | Cocaine aptamer 3′ fragment and 5′ fragment+AuNPs+CP | Cocaine aptamer 3′ fragment and 5′ fragment+Cocaine+AuNPs+CP | Cocaine aptamer 3′ fragment and 5′ fragment+ATP+AuNPs+CP |
| Color | Blue Probe | Red Probe+Target | Blue Probe+Control |

## Table S3. The assay of Thrombin aptamer

| | Step 1. Solution 1 | | |
|---|---|---|---|
| | Thrombin aptamer | Thrombin aptamer+Thrombin | Spiegelmer+Thrombin |
| Color | Colorless | Colorless | Colorless |
| | Step 2. Adding solution 1 to AuNPs solutions to make solution 2 | | |
| | Thrombin aptamer+AuNPs | Thrombin aptamer+Thrombin+AuNPs | Spiegelmer+Thrombin+AuNPs |
| Color | Red | Red | Red |
| | Step 3. Adding conjugated polyelectrolyte (CP) into solution 2 | | |
| | Thrombin aptamer+AuNPs+CP | Thrombin aptamer+Thrombin+AuNPs+CP | Spiegelmer+Thrombin+AuNPs+CP |
| Color | Blue Probe | Red Probe+Target | Blue Control+Target |

**Table S4. The assay for mercury ions**

| | Step 1. Solution 1 | | |
|---|---|---|---|
| Color | MSO probe<br>Colorless | MSO probe+Mercury ion<br>Colorless | Control sequence+Mercury ion<br>Colorless |
| | Step 2. Adding solution 1 to AuNPs solutions to make solution 2 | | |
| Color | MSO probe+AuNPs<br>Red | MSO probe+Mercury ion+AuNPs<br>Red | Contro sequence+Mercury ion+AuNPs<br>Red |
| | Step 3. Adding conjugated polyelectrolyte (CP) into solution 2 | | |
| Color | MSO probe+AuNPs+CP<br>Blue<br>Probe | MSO probe+Mercury ion+AuNPs+CP<br>Red<br>Probe+Target | Contro sequence+Mercury ion+AuNPs+CP<br>Blue<br>Control+Target |